Journal of Biomedical Optics

BiomedicalOptics.SPIEDigitalLibrary.org

Development of ultraviolet- and visible-light one-shot spectral domain optical coherence tomography and *in situ* measurements of human skin

Heijiro Hirayama
Sohichiro Nakamura

SPIE.

Development of ultraviolet- and visible-light one-shot spectral domain optical coherence tomography and *in situ* measurements of human skin

Heijiro Hirayama* **and Sohichiro Nakamura**
Analysis Technology Center, R&D Management Headquarters, Fujifilm Co., 210 Nakanuma, Minami-Ashigara-shi, Kanagawa 250-0193, Japan

Abstract. We have developed ultraviolet (UV)- and visible-light one-shot spectral domain (SD) optical coherence tomography (OCT) that enables *in situ* imaging of human skin with an arbitrary wavelength in the UV–visible-light region (370–800 nm). We alleviated the computational burden for each color OCT image by physically dispersing the irradiating light with a color filter. The system consists of SD-OCT with multicylindrical lenses; thus, mechanical scanning of the mirror or stage is unnecessary to obtain an OCT image. Therefore, only a few dozens of milliseconds are necessary to obtain single-image data. We acquired OCT images of one subject's skin *in vivo* and of a skin excision *ex vivo* for red (R, 650 ± 20 nm), green (G, 550 ± 20 nm), blue (B, 450 ± 20 nm), and UV (397 ± 5 nm) light. In the visible-light spectrum, R light penetrated the skin and was reflected at a lower depth than G or B light. On the skin excision, we demonstrated that UV light reached the dermal layer. We anticipated that basic knowledge about the spectral properties of human skin in the depth direction could be acquired with this system. © *2015 Society of Photo-Optical Instrumentation Engineers (SPIE)* [DOI: 10.1117/1.JBO.20.7.076014]

Keywords optical coherence tomography; ultraviolet–visible-light; human skin; melanin; hemoglobin.

Paper 150154R received Mar. 13, 2015; accepted for publication Jun. 12, 2015; published online Jul. 29, 2015.

1 Introduction

It is important to evaluate the appearance and health of human skin in the fields of cosmetics and medicine. Skin consists of the stratum corneum, epidermis, dermis, and hypodermis. Melanin is in the epidermis, and hemoglobin is in the blood capillaries in the dermis. It is beneficial to clarify the relationship between structures in the skin and its appearance for the development of cosmetics and the fundamental study of skin. Moreover, it is important to clarify the propagation of ultraviolet (UV) light, which is ascribed as the cause of skin damage. By cutting the skin, we can evaluate its structure with stained skin and the penetration depth of light into the skin from transmittance spectra.[1] However, it is difficult to evaluate human skin without injuring it. A nondestructive measurement is needed to measure the distinctions between each person and the effects of the application of cosmetic or pharmaceutical products.

A method based on the diffused spectral reflectivity was reported to spectroscopically analyze the spatial distributions of melanin and hemoglobin in human skin.[2] The spatial distribution of melanin and hemoglobin can be obtained by assuming a value for the optical constant of the skin. Techniques for nondestructively observing a tomogram of skin include: magnetic resonance imaging, supersonic waves, x-ray computed tomography, and optical coherence tomography (OCT). Among these, OCT is the best method to observe the stratum corneum (approximately 10-μm thickness), the epidermis (100-μm thickness), and the superior part of the upper layer of the dermis (300-μm thickness) at an appropriate resolution. OCT is an imaging method using light interference.[3–6] OCT was developed in the 1990s and has been applied to an examination of the fundus. As for the source of light, near-infrared (NIR) light (1.3 μm) is mainly used. It has been reported that the OCT image changes when a cosmetic product is applied to human skin in real time.[7] However, the use of visible light is preferred instead of NIR light to evaluate the appearance and impression of a person.

In recent years, the OCT using visible light has been reported. Full-field (FF) OCT using red (R), green (G), and blue (B) light-emitting diode light sources was reported, which measures the application thickness of foundation and the change in the reflection of each color caused by the application of foundation.[8] It is necessary to operate a sample stage for measurement by FF-OCT; thus, a skin replica was substituted. In other reports, *in vivo* human skin images were obtained by FF-OCT with a high resolution (approximately 1 μm).[9] It is necessary to physically maintain the same measurement point in human skin with a cover glass during the measurement. With the application of moisturizer, the refractive-index matching between the stratum corneum and the cover glass changed, and the imaging depth of tomography increased. It is difficult to evaluate the skin with cosmetics in its natural state because of the cover glass. Only red–NIR light was used for measurement, and images with B and G light were not obtained. In other reports, an *in vivo* albino mouse was measured by Fourier-domain (FD) OCT (SD-OCT) with a broadband visible-light source and after the measurement, the data were spectrally dispersed to each color with a calculation.[10] In the blue-light region, the short wavelength side (approximately 400 nm near the UV region) was not measured. The measurement of

*Address all correspondence to: Heijiro Hirayama, E-mail: heijiro.hirayama@fujifilm.com

1083-3668/2015/$25.00 © 2015 SPIE

a human finger by SD-OCT using a superluminescent diode with wavelengths of 680, 840, or 930 nm has been reported.[11] In another report, a broadband visible–NIR light source was used without spectroscopic dispersion to achieve a high depth resolution.[12] Therefore, there are no reports on visible-light OCT for the systematic evaluation of a tomogram of human skin with RGB light owing to a problem with the method of measurement of OCT and the wavelength range of the light source. In addition, there are no reports on OCT of human skin within the UV-light region.

In this report, we developed a system to obtain OCT images of human skin nondestructively using light in the UV–visible (370–800 nm) range with a color filter and one-shot OCT.[13,14] We obtain the tomograms for R, G, B, and UV lights of human skin.

2 Method

2.1 *System*

The optical system for UV- and visible-light one-shot SD-OCT is shown in Fig. 1. The light source (an ultrabroadband supercontinuum laser, SC400, Fianium) has a wavelength ranging from 370 to 2400 nm, a pulse width of 6 ps, and a repetition rate of 40 MHz. Light is fixed at the central wavelength of any visible level and with wavelength width by a color filter. The source light beam is split into two beams—the sample light beam and reference light beam—by a quartz substrate beamsplitter. The sample light beam is linearly focused on human skin by an achromatic cylindrical lens (CL1). We use CL3 behind the quartz substrate for the object lens in the y direction of human skin. We use a beam expander (BE) to improve the resolution in the y direction by increasing the magnification ratio of the image. Light propagates into the spectrometer through an image lens. The two-dimensional (2-D) signal in the y direction of human skin and the spectrum is obtained by a spectroscope and a 2-D charge-coupled device. We adopt SD-OCT in this system. The optical power of the detected interference light is expressed as follows:[15,16]

$$I(k) = I_r(k) + 2\sqrt{I_s(k)I_r(k)}\sum_n \alpha_n \cos(kz_n) + I_s(k), \tag{1}$$

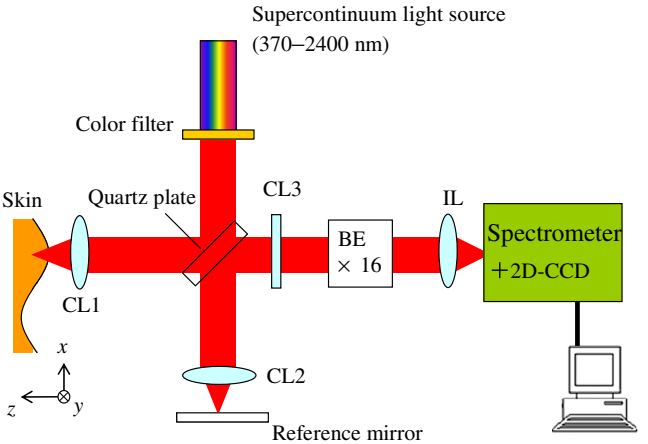

Fig. 1 Ultraviolet(UV)- and visible-light one-shot spectral domain optical coherence tomography (SD-OCT) system.

where $I_s(k)$ and $I_r(k)$ are the wavenumber-dependent intensities of the sample and reference light beams, respectively, and k is the wavenumber. The second term on the right-hand side of Eq. (1) represents the interference between the sample and reference light beams. α_n is the square root of the sample reflectivity at the depth z_n. The information in the depth direction of the sample is obtained by an inverse Fourier transform of Eq. (1) as

$$|\mathrm{FT}^{-1}[I(k)]|^2 = \Gamma^2(z) \otimes \left\{\delta(0) + \sum_n \alpha_n^2 \delta(z - z_n) + \sum_n \alpha_n^2 \delta(z + z_n) + O[I_s^2/I_r^2]\right\}, \tag{2}$$

where $\Gamma(z)$ represents the envelope of the coherence function. The first term in the curly braces expresses the autocorrelation function of the reference light. The second and third terms express the interference of the sample light and reference light, which gives us information related to the depth direction in the sample. The fourth term expresses the autocorrelation function noise. The system, consisting of SD-OCT with multicylindrical lenses, allows us to obtain a single image by a one-shot measurement whose time is only a few dozens of milliseconds. Therefore, we can nondestructively and noninvasively obtain a tomogram of human skin.

2.2 *System Performance*

Figure 2 shows the spectrum of light that was used for the OCT measurement of human skin in this study. The wavelengths of the R, G, B, and UV lights are 650 ± 20, 550 ± 20, 450 ± 20, and 397 ± 5 nm, respectively. The light intensity is approximately 1 mW/cm^2 for R, G, or B light and approximately 5 μW/cm^2 for UV light. The depth resolution for OCT is given by $2 \times [\ln(2)/\pi] \times (\lambda^2/n\Delta\lambda)$ in theory, where λ is the

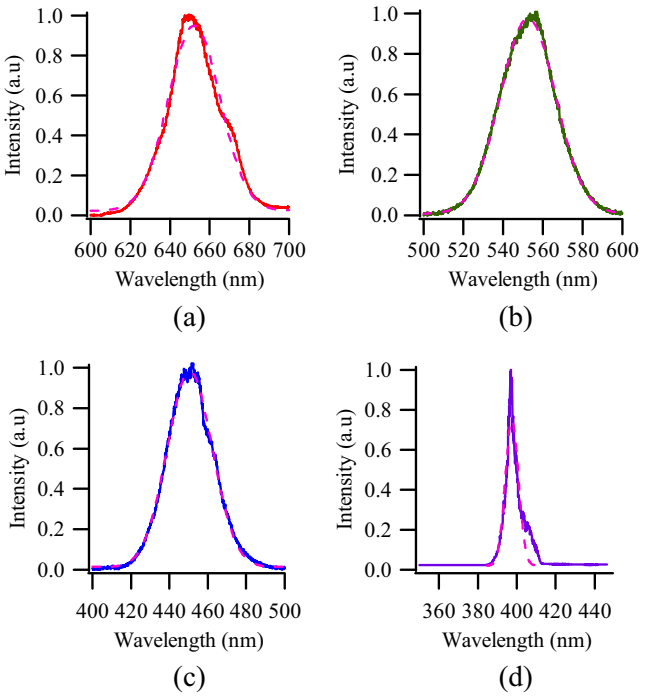

Fig. 2 Light spectra transmitted by a single-color transmittance filter: (a) R, (b) G, (c) B, and (d) UV light.

central wavelength, n is the refractive index, and $\Delta\lambda$ is the spectrum width of the light source. The depth resolution improves as λ is decreased or $\Delta\lambda$ is increased. The theoretical depth resolution in air was 9.3, 6.7, 4.5, and 14 μm in reference to R light, G light, B light, and UV light, respectively. The transverse resolution was approximately 6 μm, which was acquired from an USAF 1951 resolution target.

3 Results

3.1 *Validation*

Figure 3 shows the absolute-squared interferograms of light, which were obtained by a fast Fourier transform of the spectra in Fig. 2. The half bandwidth for the peak in air was 7.7 μm in reference to R light, 5.3 μm in reference to G light, and 3.6 μm in reference to B light. We accurately estimated the depth resolution for R, G, and B light almost as planned. As for UV light, the half bandwidth for peak in Fig. 3 was 5.0 μm, which was very narrow compared to the theoretical depth resolution. Meanwhile, the bottom of the spectrum in Fig. 3 was broad. This was thought to be due to the deviation in the UV light spectrum in Fig. 2 from an ideal Gaussian distribution.

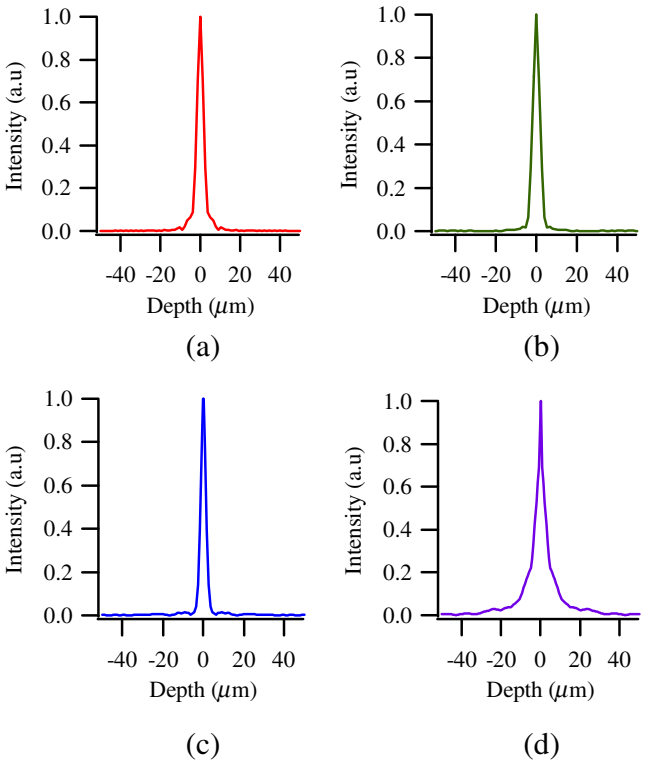

Fig. 3 Absolute-squared interferograms of the light spectra in Fig 2: (a) R, (b) G, (c) B, and (d) UV light.

Figure 4 shows an example measurement of a multilayered film with R light (698 $\pm$ 32 nm). We measured the reflection of light from the surface, boundary faces, and reverse face of the film. Assuming that the refractive index of the sample is 1.5, the half bandwidth for the peak in Fig. 4(c) was estimated to be ~4 μm, which is approximately the same as the theoretical resolution with R light (698 $\pm$ 32 nm). The maximum measurement depth was approximately 600 μm. The measurement time was 100 ms on average because the sample did not move during the measurement.

3.2 *Red Green Blue Tomography of Live Human Skin*

Figure 5 shows a tomogram of live human skin (the back of the left arm, skin phototype III, 36 years old) for each RGB color. The measurement time was 20 ms. For a comparison of the tomograms of each color, the brightness of each tomogram was divided by the peak intensity of the spectrum of the laser source with each color filter in Fig. 6 for normalization. The peak intensities depended on the overall system performance including the intensity of the laser source, the transmittance of the color filter, and the sensitivities of the spectroscope and detector. In Fig. 5, we can observe an irregularity in the skin surface and the stratum corneum, the epidermis, and the upper layer of the dermis.[17] The imaging depth of R light was greater than 200 μm in Fig. 5(a). The signal from the dermis is higher than that from the epidermis because of the large scattering of light by fibrous tissue such as collagen in the dermis. The signal of the G light was mainly observed within the depth of approximately 150 μm from the surface of the skin in Fig. 5(b). The signal of the G light from the dermis was smaller than the signal of the R light from the dermis because G light was absorbed by the hemoglobin in the blood capillaries in the dermis. B light was mainly reflected from a depth of less than 100 μm in Fig. 5(c). This is mainly because B light is absorbed by the melanin in the epidermis, which has a larger coefficient of

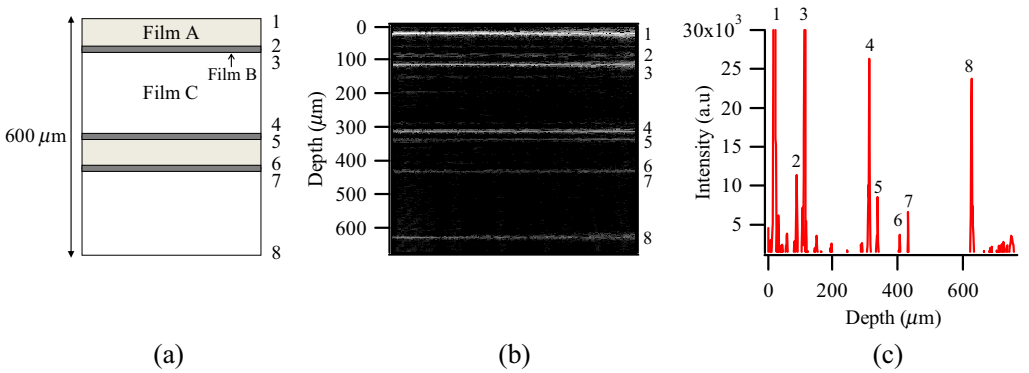

Fig. 4 Example measurement of a multilayered film. (a) Schematic of the film. The numbers indicate the boundaries. (b) Tomogram of the film. The brightness corresponds to a logarithmic scale. (c) One-dimensional profile of the tomogram.

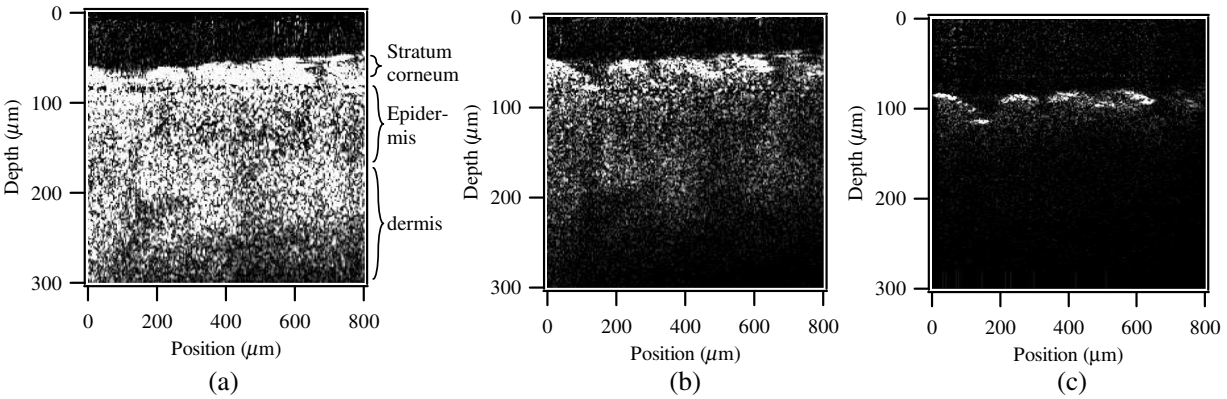

Fig. 5 RGB tomography of live human skin: (a) R light (650 ± 20 nm), (b) G light (550 ± 20 nm), and (c) B light (450 ± 20 nm). The brightness corresponds to a linear scale.

absorption in the wavelength region of B light than G and R light. To our knowledge, these are the first tomographic images of live human skin with R, G, and B lights. This makes it possible to discuss the differences in the imaging depth of each color. We attributed the differences in the imaging depth to the absorption by the pigment cells in human skin.[18,19]

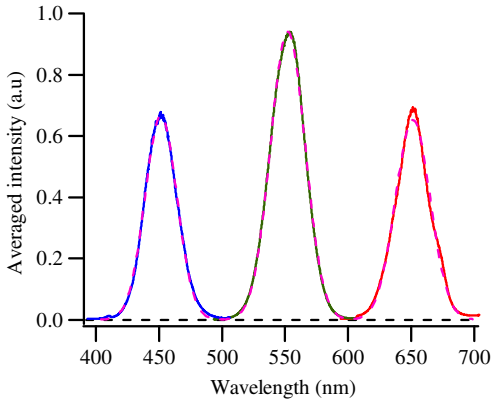

Fig. 6 Spectra of the laser source with each color filter. The intensity of each position (*y*-direction) was averaged. The dashed line is the Gaussian curve.

R light deeply penetrated the skin and was reflected from various depths in the skin. Therefore, in daily life, R light is considered to make mottled points and wrinkles on the surface of the skin less noticeable by the soft focusing effect in the depth direction. On the other hand, B light was reflected from the skin at more shallow depths. Therefore, B light is considered to emphasize mottled points and wrinkles on the surface of the skin.

3.3 *Ultraviolet Tomography of a Skin Excision*

The entire protocol was approved by the institutional review board at the Fujifilm Co. Figure 7(a) shows a stained skin excision (female, Caucasian, abdomen, 38 years old, BIOPREDIC). The epidermal thickness was approximately 100 μm. A tomogram of the skin excision with UV light (397 ± 5 nm) is shown in Fig. 7(b). The locations of measurement for Figs. 7(a) and 7(b) are different. The intensity of the UV light is much smaller than the visible-light intensity, so we removed BE in Fig. 1 to increase the detected intensity. The resolution in the *y* direction decreased as the detected intensity increased. We changed the grating of the spectrometer from 1200 to 2400 L/mm to increase the measurement depth by improving the wavelength

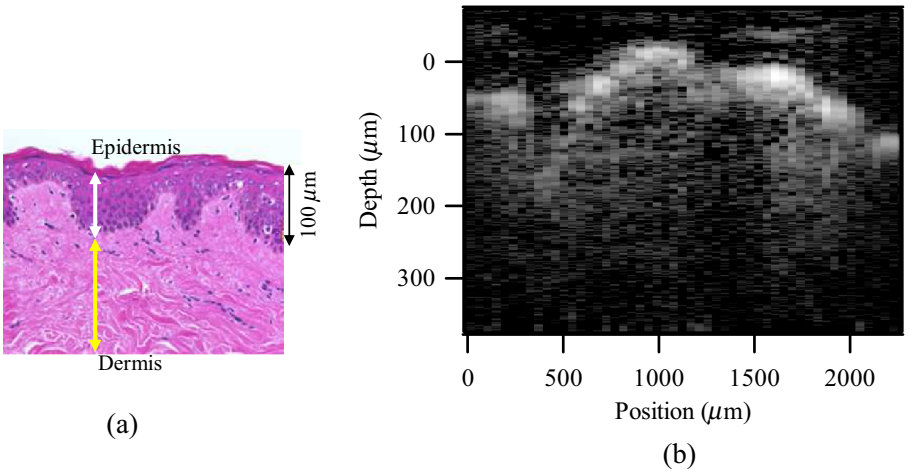

Fig. 7 (a) Stained skin excision. (b) Tomogram of the skin excision, which is the same as (a) with UV light (397 ± 5 nm). The locations of measurement for (a) and (b) are different. The brightness corresponds to a logarithmic scale.

resolution. The intensity of the UV light is much smaller than the intensity of sunlight.

In Fig. 7, scattered light from a depth of approximately 200 μm from the surface of the skin was observed. On one subject, we demonstrated that UV-A light reached the dermis with tomography. UV-A light (320–400 nm) is said to reach the dermis and causes aging such as the appearance of creases.[20] The penetration depth was simulated with various laser wavelengths and skin model types.[21,22] In the simulation, for fair or very fair skin, less than 15% of the UV-A light (365 nm) was simulated to penetrate a depth of 200 μm.[22] The OCT system could detect light that penetrated a depth of 200 μm, decayed to less than 15% in intensity, and scattered back. When the epidermal thickness was assumed to be 100 μm, the relative intensity integrated over the entire dermis and the total amount of backscattered light was calculated to be approximately 20%. The simulated transmittance of the skin heavily depends on the skin type, so we need to measure the various skin types in detail.

4 Conclusion

We developed one-shot SD-OCT that allows for nondestructive observation of a tomogram of human skin for each wavelength region of the UV–visible-light (370–800 nm) spectrum. The OCT images of human skin for R, G, B, and UV lights were measured. In the visible-light spectrum, R light penetrated the skin and was reflected from a lower depth than G or B light. R light is considered to make mottled points and wrinkles on the surface of the skin less noticeable. On the other hand, B light is considered to emphasize the mottled points and wrinkles on the surface of the skin. On one subject, we demonstrated that UV light (397 ± 5 nm) reached the dermis of the skin with tomography.

The system consists of SD-OCT with multicylindrical lenses; it takes only a few dozens of milliseconds to obtain a single image. Therefore, there is no need to physically maintain the same measurement point in human skin during the measurement. We anticipated that we could evaluate the effect of the application of cosmetics and pharmaceutical products to human skin.

References

1. W. A. G. Bruls et al., "Transmission of human epidermis and stratum corneum as a function of thickness in the ultraviolet and visible wavelengths," *Photochem. Photobiol.* **40**(4), 485–494 (1984).
2. I. Nishidate et al., "Estimation of melanin and hemoglobin using spectral reflectance images reconstructed from a digital RGB image by the Wiener estimation method," *Sensors* **13**(6), 7902–7915 (2013).
3. M. E. Brezinski, *Optical Coherence Tomography: Principles and Applications*, Academic Press, Massachusetts (2006).
4. S. K. Nadkarni et al., "Measurement of collagen and smooth muscle cell content in atherosclerotic plaques using polarization-sensitive optical coherence tomography," *J. Am. Coll. Cardiol.* **49**(13), 1474–1481 (2007).
5. Z. Wang et al., "Assessment of dermal wound repair after collagen implantation with optical coherence tomography," *Tissue Eng. Part C Methods* **14**(1), 35–45 (2008).
6. T. Gambichler et al., "*In vivo* data of epidermal thickness evaluated by optical coherence tomography: effects of age, gender, skin type, and anatomic site," *J. Dermatol. Sci.* **44**(3), 145–152 (2006).
7. S. H. Han et al., "OCT monitoring of cosmetic creams in human skin in vivo," *Proc. SPIE* **8207**, 82070W (2012).
8. R. Kimura, T. Iwai, and T. Tsugita, "Optical characterization of facial foundation applied to skin replicas by using visible FF-OCT," *Proc. SPIE* **9232**, 92320X (2014).
9. E. Dalimier et al., "High resolution *in vivo* imaging of skin with full field optical coherence tomography," *Proc. SPIE* **8926**, 89260P (2014).
10. F. E. Robles et al., "Molecular imaging true-colour spectroscopic optical coherence tomography," *Nat. Photonics* **5**, 744–747 (2011).
11. J. B. Eom, E. J. Min, and B. H. Lee, "Visible and near infrared wavelength photonic crystal fiber splitter for multiwavelength spectral domain optical coherence tomography," *Proc. SPIE* **8264**, 82641F (2012).
12. B. Povazay et al., "Submicrometer axial resolution optical coherence tomography," *Opt. Lett.* **27**, 1800–1802 (2002).
13. S. Nakamura and H. Hirayama, "Development of one shot visible spectral domain OCT," in *Proc. 61st Japan Society of Applied Physics Spring Meeting*, 17a-E6-2 (2014).
14. H. Hirayama and S. Nakamura, "Development of one shot visible spectroscopic SD-OCT and in-situ measurements of human skin," in *Proc. 39th Optical Symp.*, p. 7 (2014).
15. N. A. Nassif et al., "*In vivo* high-resolution video-rate spectral-domain optical coherence tomography of the human retina and optic nerve," *Opt. Express* **12**, 367–376 (2004).
16. G. Hausler and M. W. Lindner, "'Coherence radar' and 'spectral radar'—new tools for dermatological diagnosis," *J. Biomed. Opt.* **3**(1), 21–31 (1998).
17. R. A. Hogg and P. Andersen, "Quantum-dot diodes provide sources for optical coherence tomography," *SPIE Newsroom* (2006).
18. T. Lister et al., "Optical properties of human skin," *J. Biomed. Opt.* **17**(9), 090901 (1998).
19. A. N. Bashkatov et al., "Optical properties of human skin, subcutaneous and mucous tissues in the wavelength range from 400 to 2000 nm," *J. Phys. D: Appl. Phys.* **38**, 2543 (2005).
20. Y. Matsumura and H. N. Ananthaswamy, "Toxic effects of ultraviolet radiation on the skin," *Toxicol. Appl. Pharmacol.* **195**(3), 298–308 (2004).
21. M. Meinhard et al., "Wavelength-dependent penetration depths of ultraviolet radiation in human skin," *J. Biomed. Opt.* **13**(4), 044030 (2008).
22. F. H. Mustafa et al., "Comparison of wavelength-dependent penetration depths of lasers in different types of skin in photodynamic therapy," *Indian J. Phys.* **87**(3), 203–209 (2012).

Heijiro Hirayama finished his master's degree at the Graduate School of Engineering, Osaka University, in 2009. He joined Fuji Film Co., Ltd. He studied the spectroscopy of functional films and functional materials.

Sohichiro Nakamura finished his master's degree at the Graduate School of Arts and Sciences, The University of Tokyo, in 2002. He joined Fuji Photo Film Co., Ltd. He studied the optical measurement of functional materials and materials in the healthcare field.